Published in final edited form as:
Biomaterials. 2007 June ; 28(16): 2638–2645. doi:10.1016/j.biomaterials.2007.02.010.

Biocompatibility of nanoporous alumina membranes for immunoisolation

Kristen E. La Flamme[1], **Ketul C. Popat**[2], **Lara Leoni**[3], **Erica Markiewicz**[3], **Thomas J. LaTempa**[4], **Brian B. Roman**[3], **Craig A. Grimes**[4], and **Tejal A. Desai**[1,2,*]

[1]Department of Biomedical Engineering, Boston University, Boston, Massachusetts, 02215

[2]Department of Physiology and Division of Bioengineering, University of California San Francisco, San Francisco, CA, 94158

[3]Department of Radiology, University of Chicago, Chicago, Illinois, 60637

[4]Department of Electrical Engineering and Biomedical Engineering, The Pennsylvania State University, University Park, Pennsylvania, 16802

Abstract

Cellular immunoisolation using semi-permeable barriers has been investigated over the past several decades as a promising treatment approach for diseases such as Parkinson's, Alzheimer's, and Type 1 diabetes. Typically, polymeric membranes are used for immunoisolation applications; however, recent advances in technology have led to the development of more robust membranes that are able to more completely meet the requirements for a successful immunoisolation device, including well controlled pore size, chemical and mechanical stability, non-biodegradability, and biocompatibility with both the graft tissue as well as the host. It has been shown previously that nanoporous alumina biocapsules can act effectively as immunoisolation devices, and support the viability and functionality of encapsulated β cells. The aim of this investigation was to assess the biocompatibility of the material with host tissue. The cytotoxicity of the capsule, as well as its ability to activate complement and inflammation was studied. Further, the effects of PEG-modification on the tissue response to implanted capsules were studied. Our results have shown that the device is non-toxic and does not induce significant complement activation. Further, *in vivo* work has demonstrated that implantation of these capsules into the peritoneal cavity of rats induces a transient inflammatory response, and that PEG is useful in minimizing the host response to the material.

Keywords

bioartificial pancreas; cell encapsulation; alumina; biocompatibility

1. Introduction

The encapsulation of living metabolic cells within a semi-permeable membrane has been studied over the last 30 years as a potential treatment for a number of diseases [1–4]. It has

*Corresponding Author: tejal.desai@ucsf.edu, Fax: 1-415-514-4503.

been shown that immunoprotected cells such as pancreatic islets or hepatocytes can respond physiologically both *in vitro* and *in vivo* in response to appropriate stimuli [5–7].

However, the requirements for a successful immunoisolation device have proven difficult to achieve. The semi-permeable membrane must exhibit a well controlled pore size, chemical and mechanical stability, and biocompatibility with both the graft tissue as well as the host [8–10]. Polymeric microcapsules, such as alginate-poly L-lysine beads, are most commonly used. [11–13]. While polymeric membranes are biocompatible, easy to fabricate and have a long history of use in immunoisolation procedures; there are several disadvantages associated with them. Polymeric membranes have previously demonstrated poor chemical resistance, mechanical stability, and broad pore size distributions, all of which lead to the eventual destruction of the transplanted cells. Also, polymeric microcapsules have poor retrievability and can form aggregates in vivo which reduce their effectiveness [5, 8–10, 14–17]. Thus, there is a need to develop more robust membranes that can be used for immunoisolation applications such as those made from biocompatible inorganic materials. Inorganic membranes are much more chemically and mechanically stable, and important features such as the pore size and pore size distribution can be easily controlled by varying the fabrication parameters [5, 8–10, 14–17]. Further, the surface of inorganic membranes can be chemically tailored to resist the adhesion of blood proteins and immune cells that may block the pores and reduce the diffusion of therapeutic agents [18, 19].

In this study, we have evaluated the biocompatibility of aluminum oxide nanoporous membranes for use in immunoisolation applications. Aluminum oxide is a bioinert material that has been utilized in numerous biomedical applications such as bone prostheses, dental implants, and artificial eye sockets [20–23]. Through a simple two-step anodization process, physically strong membranes with an organized array of pores can be fabricated. We have shown previously that these biocapsules are effective as immunoisolation devices under *in vitro* conditions, and are capable of supporting the viability and functionality of insulin secreting cells [24]. However, for successful implementation, the material must be compatible with the host, eliciting a minimal, if any, foreign body reaction and complement activation. In this work, we studied the cytotoxic effects of alumina capsules, their ability to activate complement, as well as their *in vivo* inflammatory capability. Additionally, the effect of modifying nanoporous alumina with poly (ethylene glycol) (PEG) to reduce protein adsorption and improve biocompatibility was examined.

2. Methods

2.1 Fabrication

The fabrication of nanoporous alumina capsules has been described in detail elsewhere [25]. Briefly, an aluminum tube (99.9% pure), Alfa-Aesar, Ward Hill, MA) with starting length, outer diameter, and wall thickness of 2.5cm, 6.35mm, and 710 μm, respectively, was cleaned and pre-coated with a resist on the outer surface to protect it from being anodized during the subsequent fabrication steps. The inner surface of the tube was then anodized with a voltage of 60V in a solution of 0.25M oxalic acid for 8 hours. The resulting thin film of aluminum oxide (AO) was then etched away using a solution of 4 wt% chromic acid and 8 vol% phosphoric acid, leaving a pretextured aluminum surface necessary for the formation of an organized nanoarray of pores during the second anodization step. The inner side of the tube was anodized a second time under the same conditions, resulting in a layer of nanoporous alumina that serves as the final membrane. A small area of the resist on the outer surface of the tube was then removed, and the aluminum layer was etched away with a solution of 10 wt% HCl and 0.1 M $CuCl_2$. Finally, a superficial amorphous barrier layer of alumina is etched away using 10 vol% phosphoric acid, exposing the underlying nanoporous alumina. The mean pore size of these membranes was approximately 75nm; however, it

should be noted that other pore sizes can be obtained by changing the anodization voltage, with a correlation of ~1.29 nm/V. Since the membranes are actually incorporated into the tube, they are strong enough for easy handling and use, withstanding up to 32.6 MPa before failure [26]. Figure 1(a) shows the schematic of the fabrication process and Figure 1(b) shows an SEM image of a nanoporous alumina membrane with a mean pore diameter of 75nm.

2.2 Immobilization of poly (ethylene glycol) (PEG) on the biocapsules

Poly (ethylene glycol) (PEG) immobilization on the alumina surface was achieved using a covalent coupling technique described by Popat et al [18, 19]. This technique forms more stable films compared to physical adsorption on the surface. In this technique, a PEG-silane couple is formed by reacting PEG with silicon tetrachloride in presence of triethylamine as a catalyst. The reaction results in the formation of PEG-$OSiCl_3$ which then reacts with trace levels of –OH on the alumina membrane to form a network of Si-O-Si bonds, resulting in immobilization of PEG on the surface (Figure 2). The PEG-silane couple formation and its immobilization on the membranes was performed in anhydrous conditions to prevent hydrolysis and undesired side reactions. In brief, PEG (MW=1000) was dissolved in anhydrous toluene to form a PEG solution with a concentration of 10mM. Then, 0.975mmol of triethylamine was added drop by drop to the PEG solution at 25° C. The above reaction mixture was mildly shaken for one hour. Next, 0.175mmol of silicon tetrachloride was added and the reaction mixture was further shaken for 15 minutes at room temperature. The reaction mixture was then filtered through a sintered glass funnel and the filtrate was used directly to immobilize PEG on the membranes without further purification, since an excess of unreacted PEG is not expected to have harmful effects on the silanization process. Prior to immobilization, alumina membranes were cleaned and hydrophilized by boiling them in 30% H_2O_2 and DI water. Immobilization of the PEG-silane couple with alumina membranes was carried out by immersing the capsules in the filtrate solution for 1hr. After immobilization, the membranes were rinsed thoroughly with anhydrous toluene, acetone and deionized water, and were air dried and stored in argon until further use. The modified films were then characterized using X-ray photoelectron spectroscopy (XPS).

2.3 X-ray photoelectron spectroscopy

To determine the surface composition of PEG modified and unmodified alumina membranes, XPS analysis was carried out. The alumina membranes were mounted on an XPS stage. Three spots per sample were analyzed. The analysis was conducted on a Kratos AXIS Ultra Imaging X-ray Photoelectron Spectrometer with a monochromatic Al-*Kα*-X-ray small spot source (1486.6eV) and multichannel detector. A concentric hemispherical analyzer (CHA) was operated in the constant analyzer transmission mode to measure the binding energies of emitted photoelectrons. The binding energy scale was calibrated by the $Au4f_{7/2}$ peak at 83.9eV, and the linearity was verified by the $Cu3p_{1/2}$ and $Cu2p_{3/2}$ peaks at 76.5 and 932.5eV respectively. Survey spectra were collected from 0 to 1100eV with pass energy of 188eV, and a high-resolution scan was taken for the C1s peak with pass energy of 23.5eV. All spectra were referenced by setting the hydrocarbon C1s peak to 285.0eV to compensate for residual charging effects. Data for percent atomic composition, atomic ratios and peak fit analysis parameters were calculated using the manufacturer supplied software.

2.4 Protein adsorption

To investigate the nonfouling nature of PEG modified alumina membranes, interaction of proteins on these surfaces was studied. Unmodified and PEG-modified alumina membranes were transferred into wells of standard 6-well plates. Next, 2 mL of FITC-albumin solution (1 mg/mL) in phosphate buffered saline (PBS) were added to the well. Adsorption was allowed to proceed in an incubator (5 % CO_2) for 1h at 37° C. Upon completion of

adsorption, the membranes were thoroughly washed three times with deionized water for removal of non-adsorbed proteins and salts from the buffer. Fluorescence images were taken using a CCD camera attached to a microscope and fluorescence intensity on the surfaces was calculated using image processing software.

2.5 *In vitro* cytotoxicity test

Sterilized capsules were fixed into the bottom of each well of a 6 well tissue culture plate with Dow Corning Silcone Type A medical adhesive. A drop of silicone adhesive was used as a positive control whereas latex with approximately the same surface area as the capsule was used as a negative control. Approximately 500,000 IMR-90 lung fibroblasts were seeded into each well along with Modified Eagle Medium (supplemented with 10% fetal bovine serum and 1% penicillin streptomycin) and incubated at 37°C with 5% CO_2. After 24 hours, the cells were trypsinized from each well and stained with Trypan Blue dye. The viable cells were counted using a hemacytometer. The extent of cytotoxicity was determined by comparing the final number of viable cells to the initial number of cells seeded.

2.6 Complement Activation

Sterilized capsules were placed in each well of a 6 well tissue culture plate and immersed in complement preserved human serum (Bioreclamation, Hicksville, NY) for 7 days. As a positive control, zymosan A, a cell wall polysaccharide of yeast that is known to cause complement activation, was added to the serum at a concentration of 2.5 mg/mL; and as a negative control, serum alone was incubated in the well. Samples of 100 μL were taken after 1, 4, and 7 days, and 12 μL of Na_2EDTA were added to each to prevent any further complement activation. Samples were stored at −80°C until they were assayed. An enzyme-linked immunoassay (Quidel, San Diego, CA) was used to quantify the amount of Bb fragment in each sample, which is an indicator of activation of the alternative complement pathway.

2.7 In-vivo inflammation studies

These studies were carried out in conformity with Animal Care and Use Procedures at University of Chicago under protocol 71690. Male Lewis rats (225 g) were anesthetized in an induction box with 3% isoflurane and then kept on 1.5% isoflurane on a fitted nose mask during the course of the surgery. Each animal was clipped and prepped following aseptic techniques described in the guidelines for lab animals. A 2cm midline incision was made in the lower abdominal region. The skin layer was detached from the muscle layer to allow for the biocapsule suturing. 4.0 silk thread was passed through each biocapsule (previously sterilized by autoclaving). Two devices (one PEG-modified, one unmodified) were implanted in each animal, one on each side of the incision, and were secured to the abdominal wall by 4.0 silk sutures. The muscle layer incision was sutured with 4.0 vicryl suture and the skin layer was then sutured with 4.0 nylon suture. The animals were allowed to recover before being returned to the animal facility. They were monitored every day for the first week and twice a week thereafter. Nylon stitches were removed after a week.

At the time of explant, each animal was anesthetized as described above. A midline incision was made in the skin layer and the skin was detached from the muscle layer. A midline incision was made in the muscle layer and the animals were euthanized by cardiac removal. Biocapsules and surrounding tissue were removed within one minute from euthanasia. A piece of tissue in the upper abdominal region was removed as a control. The tissue samples were fixed in formalin. For histological evaluation, the formalin-fixed samples were dehydrated in a graded series of reagent alcohols and embedded in paraffin wax. Samples were placed on ice for approximately 1 min and soaked in 5% ammonium water for approximately 10 minutes. The samples were cut in 4 μm sections and mounted on glass

slides. The slides were then incubated at 65°C for approximately 30 minutes. They were then deparaffinized in xylene substitute (citrus clearing solvent) and rehydrated through a series of alcohols to distilled water. The slides were then stained with hematoxylin and eosin using an automatic stainer, and the samples were examined for the signs of inflammation.

2.8 Statistics

Each experiment was reconfirmed at least three times using different cell culture preparations. All the results were analyzed using nonparametric t-test. Statistical significance was considered at $p<0.05$.

3. Results

3.1 PEG surface modification and characterization

PEG immobilized alumina membranes were prepared using the covalent coupling technique described earlier. XPS analysis was performed to ensure the presence of PEG on the surface. Table 1 shows the elemental composition of unmodified and PEG modified alumina surfaces. The survey for PEG modified membranes shows an increase in C1s (285eV) as well as decrease in Al2p (72eV) peaks compared to the unmodified surface, suggesting a PEG film on the surface (Figure 3(a)). This is further supported by the presence of a Si2p (100eV) peak on PEG modified membranes which is due to the presence of silicon in the PEG-silane couple. To further support the presence of PEG on alumina membranes, a high resolution scan of the C1s peak was taken (Figure 3(b)). There is a distinct increase in the overall intensity of the C1s peak after PEG modification. Also, the high resolution C1s peak for PEG modified membranes consists of two well defined peaks, a peak at 285eV which is the C-C peak and a second peak at a shift of 1.5ev from C-C, which is the C-O peak. The high resolution scan of a C1s peak for unmodified membranes consists of only one peak at 285eV which is the C-C peak (carbon is present on the unmodified membranes due to impurities). Presence of the C-O peak on modified membranes suggests formation of PEG films.

3.2 Protein interaction with PEG modified surfaces

The interaction of PEG modified membranes with FITC-Albumin in solution form was studied to better understand their behavior in physiological environments. Unmodified and PEG modified surfaces were incubated with FITC-albumin in PBS (1mg/ml) for 1 hr. The albumin adsorbed membranes were observed under fluorescence microscope and the fluorescence intensity was calculated using image processing software. There was 85% reduction in fluorescence intensity on PEG modified membranes as compared to the unmodified membrane suggesting non-fouling nature of PEG films (data not shown).

3.3 *In vitro* cytotoxicity Test

The results of the *in vitro* cytotoxicity test are shown in Figure 4. There was slight proliferation in the experimental case, with virtually no difference between the experimental and the positive control. On the other hand, the latex treated cells were reduced in number by about 94%.

3.4 Complement activation

To assess the influence of the capsule on complement activation, an ELISA assay was used that quantified the amount of the Bb enzyme fragment present in serum samples exposed to the material. The Bb fragment is an activation by-product of the alternative complement pathway. These results are reported in Figure 5. Zymosan-A treated serum exhibited a statistical difference with respect to the capsule treated serum ($p < .025$) at all 3 time points,

whereas there was no difference between the capsule treated serum and the negative control after 7 days.

3.5 *In-vivo* inflammation

The implanted capsules were retrieved from the inner abdominal wall after 1, 2, 3, and 4 weeks. At macroscopic examination, both the PEG-modified and unmodified capsules appeared clean, with no fibrous growth around the outside of the capsule, even after 4 weeks, and the membranes remained intact. Sample of the tissue surrounding the capsules were processed and stained with hematoxylin and eosin as described in section 2.7 and examined for signs of inflammation under a light microscope. Figure 6(a) and (d) show the images of control tissue not exposed to the capsules. After one week, there is some inflammation of the tissue surrounding the unmodified capsules as evidenced by the presence of lymphocytes and macrophages embedded in a granulation layer (Figure 6(b)). There is a similar but less severe effect in the tissue surrounding the PEG-modified capsules (Figure 6(c)). The presence of immune cells appears to recede after 4 weeks (Figure 6(e) and (f)), however, for tissue exposed to unmodified capsules, the granulation layer persists, while there appears to be a reduction in the granulation tissue for tissue exposed to PEG-modified capsules.

4. Discussion

The biocompatibility of an implantable material is determined by the severity of the reaction by the recipient. With bioartificial systems such as the one described here, induction of the foreign body response poses a serious challenge to clinical success. The major consequence of a non-biocompatible device is the development of fibrous overgrowth on the material that interferes with the supply of oxygen as well as the diffusion of biomolecules [4, 27–29].

Determining the cytotoxicity of a material is a central issue in deciding whether or not it is suitable for implantation. The *in vitro* cytotoxicity test is a standard test that provides information on the interactions between cells and the surface of the material, and is often used as an initial evaluation of biocompatibility [30–32]. Here, the viability of cells was evaluated after a 24 hour period, and no significant difference was found between the positive control and the capsules (Figure 4). In contrast, latex, which was used as a negative control, clearly exhibited a toxic effect. This data is encouraging and suggests that the material from which the device is made should not have toxic effects on the surrounding tissue.

Complement activation by a biomaterial plays an important role in the subsequent foreign body reaction [33]. Generally speaking, biomaterials tend to activate the complement system via the alternative pathway. Once a material is implanted, the spontaneous activation of the complement component C3 commences a cascade of immunological events including the lysis of cells, phagocytosis of particulate antigens, secretion of immunoregulatory molecules, and especially the recruitment of inflammatory cells such as neutrophils and macrophages that contribute to the engulfment of the device by a fibrous capsule. Therefore the assessment of complement activation by a biomaterial has been used by many groups as one measure of biocompatibility [34–37]. We quantified the extent of complement activation by nanoporous alumina capsules over a 7 day time period. As can be seen from Figure 5, there was virtually no difference in complement activation between the negative control and the experimental condition. On the other hand, serum samples exposed to Zymosan A, which is known to induce complement activation by the alternative pathway, presented significantly higher amounts of Bb, indicating complement activation.

While *in vitro* tests can give indicative results of a material's biocompatibility, *in vivo* studies give a much clearer idea of what the tissue response is like post-implantation. Numerous studies have shown that the intraperitoneal space is the implantation site of choice for devices treating diabetes, because insulin delivered in this way more closely resembles the body's natural physiology, with the insulin being taken up by the portal system and preferentially absorbed by the liver [38, 39]. Additionally, portal insulin absorption achieves faster plasma kinetics and greater reproducibility than other delivery routes such as subcutaneous injection. Thus, both PEG-modified and unmodified samples were implanted in the intraperitoneal cavity of rats. A macroscopic examination of the retrieved capsules showed no fibrous growth, even up to 4 weeks of implantation, and all membranes were fully intact. Samples of the tissue exposed to the capsule were then stained and assessed with a light microscope for signs of inflammation. Figure 6 shows the tissue effects of these capsules compared to a control, after 1 and 4 weeks of implantation. Initially, after 1 week there is moderate inflammation of the tissue surrounding both the PEG-modified and unmodified capsules, with the unmodified capsules inducing slightly more inflammation. The histological evaluation revealed the presence of macrophages and lymphocytes in a very intact granulation layer (Figure 6(c) and (d)). However, the inflammation response seems to be transient as the presence of immune cells recedes after 4 weeks. The images after 4 weeks show a reduction in the granulation layer adjacent to the tissue exposed to the PEG-modified material. Also, blood vessels are seen in the tissue treated with the PEG modified capsules. This is encouraging since it suggests that the greatest amount of inflammation would be due to the injury of the implantation procedure itself, and that the tissue surrounding the implant would be relatively undisturbed. Further, these data confirm that PEG is useful in limiting unfavorable interactions between the material and the host.

5. Conclusions

This study focused on assessing the biocompatibility of an immunoisolation macrodevice comprised of a nanoporous alumina membrane. These capsules have many appealing features for cellular encapsulation applications. The membranes are extremely durable, and important parameters such as pore size can easily be controlled. *In vitro* tests have shown that the device is non-toxic and does not induce significant complement activation. We have also shown that incorporating a poly(ethylene glycol) coating reduces the interactions of serum albumin with the material. Finally, *in vivo* work has demonstrated that implantation of these capsules into the abdominal cavity of rats induces a transient inflammatory response, and that PEG was useful in minimizing the host response.

Acknowledgments

The authors would like to thank the NIH and the NSF for partially funding this project.

References

1. Chick WL, et al. A hybird artifical pancreas. Trans Am Soc Artif Intern Organs. 1975; 21:8–15. [PubMed: 1096419]
2. Colton CK. Implantable biohybrid artificial organs. Cell Transplant. 1995; 4(4):415–36. [PubMed: 7582573]
3. Lanza RP, Chick WL. Encapsulated Cell Therapy. Sci Am Sci Med. 1995; 2:16–25.
4. Uludag H, De Vos P, Tresco PA. Technology of mammalian cell encapsulation. Adv Drug Deliv Rev. 2000; 42(1–2):29–64. [PubMed: 10942814]
5. Desai TA, Hansford D, Ferrari M. Characterization of micromachined silicon membranes for immunoisolation and bioseparation applications. J Memb Sci. 1999; 159:221–231.

6. Figliuzzi M, et al. Subcutaneous xenotransplantation of bovine pancreatic islets. Biomaterials. 2005; 26(28):5640–5647. [PubMed: 15878369]
7. Yin C, et al. Microcapsules with improved mechanical stability for hepatocyte culture. Biomaterials. 2003; 24(10):1771–80. [PubMed: 12593959]
8. Desai TA, Hansford DJ, Ferrari M. Micromachined interfaces: new approaches in cell immunoisolation and biomolecular separation. Biomol Eng. 2000; 17(1):23–36. [PubMed: 11042474]
9. Desai TA, et al. Nanopore Technology for Biomedical Applications. Biomed Microdevices. 1999; 2(1):11–40.
10. Leoni L, Boiarski A, Desai TA. Characterization of Nanoporous Membranes for Immunoisolation: Diffusion Properties and Tissue Effects. Biomed Microdevices. 2002; 4(2):131–139.
11. Chen J, et al. Microencapsulation of islets in PEG-amine modified alginate-poly(L-lysine)-alginate microcapsules for constructing bioartificial pancreas. J Ferment Bioeng. 1998; 86(2):185–190.
12. Orive G, et al. Biocompatibility of alginate-poly-L-lysine microcapsules for cell therapy. Biomaterials. 2006; 27(20):3691–700. [PubMed: 16574222]
13. Thu B, et al. Alginate polycation microcapsules. II. Some functional properties. Biomaterials. 1996; 17(11):1069–79. [PubMed: 8718966]
14. Desai TA. MEMS-based technologies for cellular encapsulation: Focus on nanopore biocapsules for diabetes mellitus therapy. Am J Drug Deliv. 2003; 1:3–11.
15. Desai TA, et al. Nanoporous microsystems for islet cell replacement. Adv Drug Deliv Rev. 2004; 56(11):1661–73. [PubMed: 15350295]
16. Leoni L, Desai TA. Micromachined biocapsules for cell-based sensing and delivery. Adv Drug Deliv Rev. 2004; 56(2):211–29. [PubMed: 14741117]
17. Tao SL, Desai TA. Microfabricated drug delivery systems: from particles to pores. Adv Drug Deliv Rev. 2003; 55(3):315–28. [PubMed: 12628319]
18. Popat KC, Desai TA. Poly(ethylene glycol) interfaces: an approach for enhanced performance of microfluidic systems. Biosens Bioelectron. 2004; 19(9):1037–44. [PubMed: 15018959]
19. Popat KC, et al. Surface modification of nanoporous alumina surfaces with poly(ethylene glycol). Langmuir. 2004; 20(19):8035–41. [PubMed: 15350069]
20. Galindo ML, et al. [Long-term clinical results with Procera AllCeram full-ceramic crowns]. Schweiz Monatsschr Zahnmed. 2006; 116(8):804–9. [PubMed: 16989114]
21. Morel X, et al. [Biocompatibility of a porous alumina orbital implant. Preliminary results of an animal experiment]. J Fr Ophtalmol. 1998; 21(3):163–9. [PubMed: 9759400]
22. Popat KC, et al. Influence of nanoporous alumina membranes on long-term osteoblast response. Biomaterials. 2005; 26(22):4516–22. [PubMed: 15722120]
23. Swan EE, Popat KC, Desai TA. Peptide-immobilized nanoporous alumina membranes for enhanced osteoblast adhesion. Biomaterials. 2005; 26(14):1969–76. [PubMed: 15576171]
24. La Flamme KE, et al. Nanoporous alumina capsules for cellular macroencapsulation: transport and biocompatibility. Diabetes Technol Ther. 2005; 7(5):684–94. [PubMed: 16241869]
25. Gong D, et al. Controlled molecular release using nanoporous alumina capsules. Biomed Microdev. 2003; 5:75–80.
26. Itoh N, et al. Strengthened porous alumina membrane tube prepared by means of internal anodic oxidation. Microporous Mesoporous Mater. 1998; 20(4–6):333–337.
27. Anderson JM. Inflammatory response to implants. ASAIO Trans. 1988; 34(2):101–7. [PubMed: 3285869]
28. Anderson JM. Biological Responses to Materials. Annu Rev Mater Res. 2001; 31:81–110.
29. Anderson, JM., et al. Host Reactions to Biomaterials and Their Evaluation. In: Ratner, BD., editor. Biomaterials. 2. San Diego: Academic Press; 1996. p. 293-303.
30. Neumann A, et al. Comparative investigation of the biocompatibility of various silicon nitride ceramic qualities in vitro. J Mater Sci Mater Med. 2004; 15(10):1135–40. [PubMed: 15516875]
31. Van Tienhoven EA, et al. In vitro and in vivo (cyto)toxicity assays using PVC and LDPE as model materials. J Biomed Mater Res A. 2006; 78(1):175–82. [PubMed: 16628708]

32. Zhang M, Desai T, Ferrari M. Proteins and cells on PEG immobilized silicon surfaces. Biomaterials. 1998; 19(10):953–60. [PubMed: 9690837]
33. Nilsson B, et al. The role of complement in biomaterial-induced inflammation. Mol Immunol. 2007; 44(1–3):82–94. [PubMed: 16905192]
34. Bosetti M, et al. In vitro evaluation of the inflammatory activity of ultra-high molecular weight polyethylene. Biomaterials. 2003; 24(8):1419–26. [PubMed: 12527283]
35. Madani F, et al. PEGylation of microspheres for therapeutic embolization: preparation, characterization and biological performance evaluation. Biomaterials. 2007; 28(6):1198–208. [PubMed: 17113637]
36. Murakami Y, et al. Interaction of poly(styrene sulfonic acid) with the alternative pathway of the serum complement system. J Biomater Sci Polym Ed. 2005; 16(3):381–95. [PubMed: 15850291]
37. Sandeman SR, et al. Assessing the in vitro biocompatibility of a novel carbon device for the treatment of sepsis. Biomaterials. 2005; 26(34):7124–31. [PubMed: 15967498]
38. Duckworth WC, Saudek CD, Henry RR. Why intraperitoneal delivery of insulin with implantable pumps in NIDDM? Diabetes. 1992; 41(6):657–61. [PubMed: 1587393]
39. Udelsman R, et al. Intraperitoneal delivery of insulin via mechanical pump: surgical implications. Langenbecks Arch Surg. 2000; 385(6):367–72. [PubMed: 11127519]

(A)

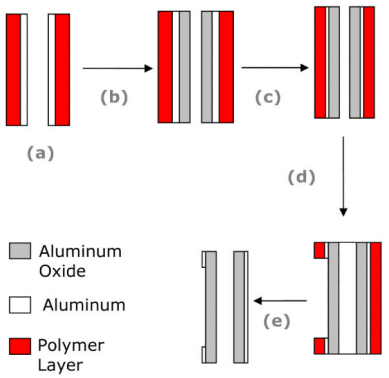

(B)

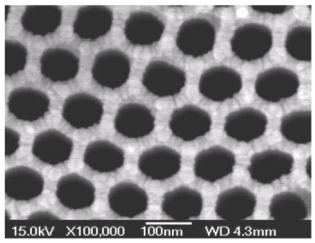

Figure 1.

Illustration of the fabrication process. (A) (a) The outer surface of an aluminum tube is coated with a protective resist; (b) The inner surface of the tube is anodized, forming a thin layer of aluminum oxide which is subsequently etched away, leaving a pretextured aluminum surface necessary for the formation of an organized pore array; (c) The inner surface of the tube is anodized a second time; (d) A small area of the resist is removed and the underlaying aluminum and barrier layer are etched away, exposing the aluminum oxide; (e) The resist on the outer surface is removed. (B) SEM image of a membrane with a pore size of ~75 nm.

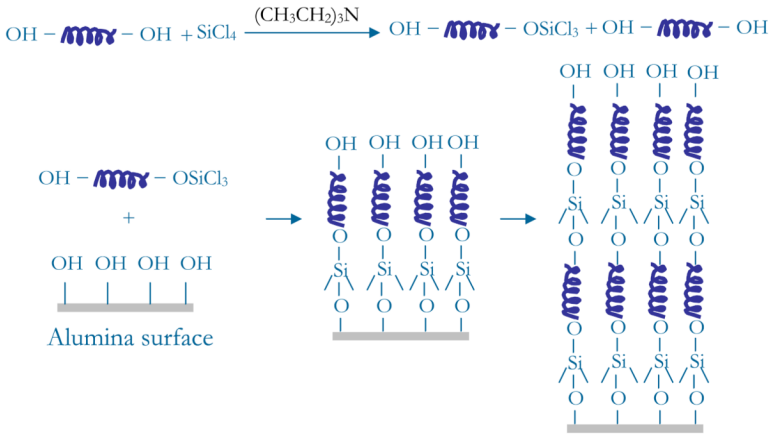

Figure 2.

Illustration of the immobilization of PEG to nanoporous alumina. In this technique, a PEG-silane couple is formed by reacting PEG with silicon tetrachloride in presence of triethylamine as a catalyst. The reaction results in the formation of PEG-$OSiCl_3$ which would then react with the trace level –OH on the alumina membrane to form a network of Si-O-Si bonds resulting in immobilization of PEG on the surface.

(A)

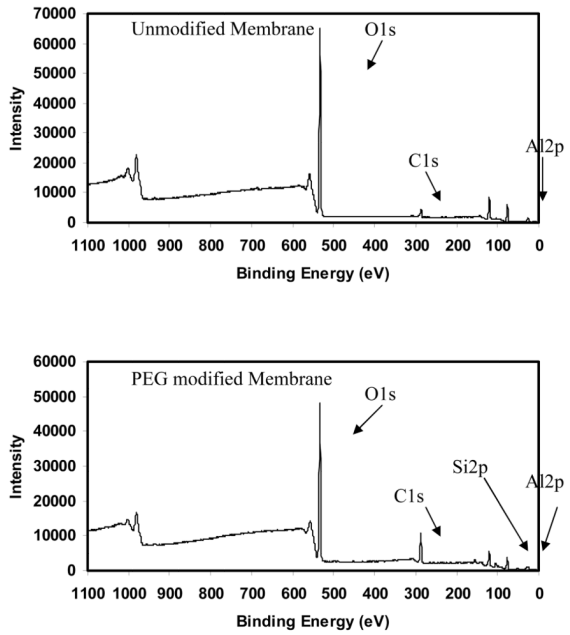

(B)

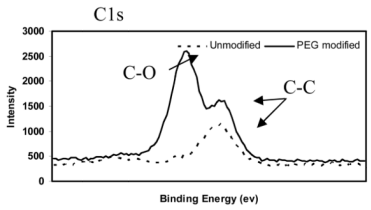

Figure 3.

(a) XPS scan data for unmodified and PEG-modified capsules. (b) High resolution XPS data for the C1s peak for both unmodified and PEG-modified alumina.

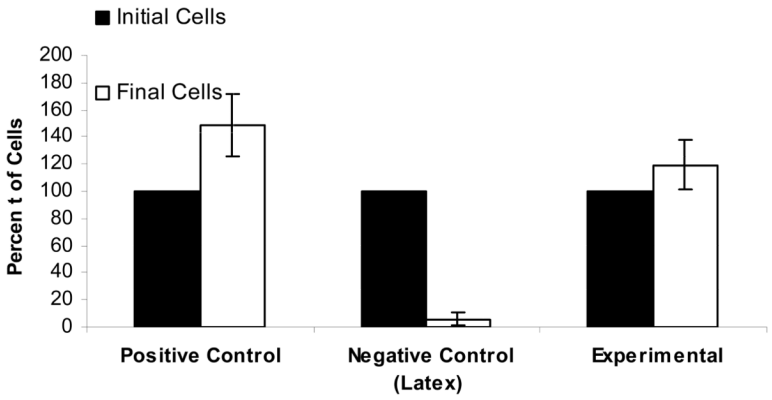

Figure 4.
In-vitro cytotoxicity test. While there is virtually no difference between the positive control and the experimental, latex, which was used as a negative control, exhibits a clear toxic effect on IMR-90 fibroblast cells.

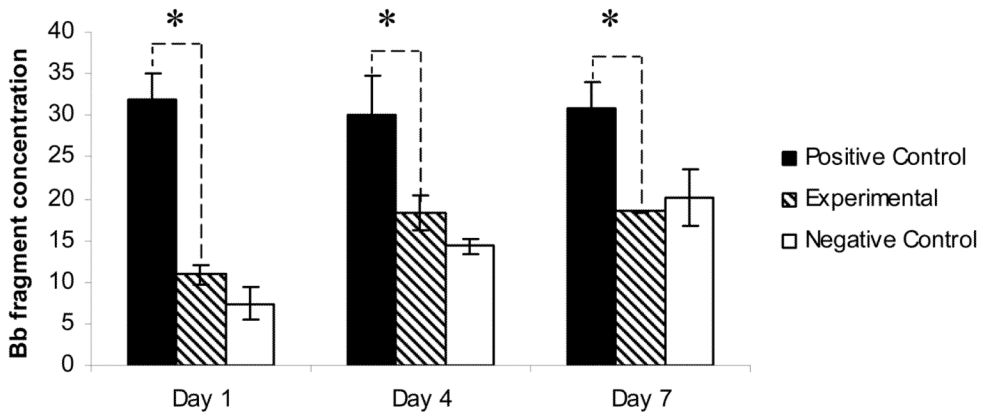

* $p<.05$

Figure 5.
Complement activation results. Even after one week, there is not significant complement activation as compared to the negative control.

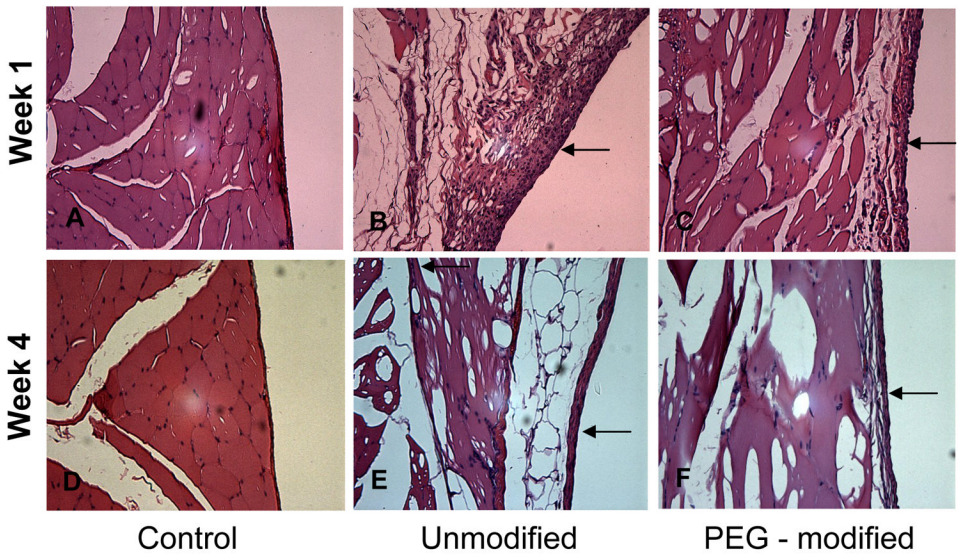

Figure 6.
Histological examination of tissue exposed to no material (A, D), unmodified capsules (B, E), and PEG-modified capsules (C, F) after 1 and 4 weeks. Arrows indicate the portion of the tissue that was exposed to the capsule.

Table 1

The elemental composition of unmodified and PEG modified alumina surfaces.

%	Al2p	Si2p	C1s	O1s
Unmodified	20.56	0	8.90	70.54
PEG modified	13.03	2.24	28.75	55.98